

WMAP Dark Matter Constraints and Yukawa Unification in SUGRA models with CP Phases

Mario E. Gómez^a, Tarek Ibrahim^{b,c}, Pran Nath^{c,d} and Solveig Skadhauge^e

*a. Departamento de Física Aplicada, Facultad de Ciencias Experimentales,
Universidad de Huelva, 21071 Huelva, Spain*

*b. Department of Physics, Faculty of Science, University of Alexandria,
Alexandria, Egypt**

c. Department of Physics, Northeastern University, Boston, MA 02115-5000, USA.

d. Max Planck Institute for Physics, Fohringer Ring 6, D-80805, Munich, Germany.

e. Instituto de Física, Universidade de São Paulo, 05315-970 São Paulo, SP, Brazil.

Abstract

The compatibility of producing the observed amount of dark matter, as indicated by the WMAP data, through the relic abundance of neutralinos with Yukawa unification and with the measured rate of $b \rightarrow s\gamma$ is analyzed in mSUGRA and extended SUGRA unified models with the inclusion of CP phases. The CP phases affect the analysis in several ways, e.g., through the threshold corrections to the b-quark mass, via their effects on the neutralino relic density and through the SUSY contribution to the $\text{BR}(b \rightarrow s\gamma)$ which is sensitive to the CP phases. We present some specific models with large SUSY phases, which can accommodate the fermion electric dipole moment constraints and give a neutralino relic density in agreement with observations as well as with the b- τ unification constraint. The possibility of achieving WMAP relic density constraints with full Yukawa unification is also explored.

*Permanent address of T.I.

1 Introduction

The Wilkinson Microwave Anisotropy Probe (WMAP) has placed stringent bounds on the amount of cold dark matter (CDM) in the universe. The amount of CDM deduced from WMAP data is given by[1, 2]

$$\Omega_{CDM}h^2 = 0.1126^{+0.008}_{-0.009} , \quad (1)$$

where $\Omega_{CDM} = \rho_{CDM}/\rho_c$, and where ρ_{CDM} is the matter density of cold dark matter and ρ_c is the critical matter density needed to close the universe, and h is the Hubble parameter measured in units of 100km/s/Mpc. It is reasonable to assume that similar amounts of dark matter exist in our Milky Way and in the terrestrial neighborhood, and there are many ongoing experiments for the detection of such dark matter in the laboratory. On the theoretical side the WMAP data on cold dark matter puts stringent constraints on unified models of fundamental interactions since such models are called upon to predict or at least accommodate the WMAP data on CDM. As is well known, supergravity unified models [3] with R-parity conservation allow for the possibility that the lightest neutralino may be the lightest supersymmetric particle (LSP) which could serve as a dark matter candidate [4]². A hallmark of many unified models is Yukawa unification. In this paper we carry out a detailed investigation of the possibility of accommodating the WMAP cold dark matter data in the neutralino LSP scenario but under the constraints of Yukawa unification and including the effect of CP phases³. Another important constraint is the FCNC constraint given by $b \rightarrow s + \gamma$ which is discussed in some detail in this paper and included in the analysis.

Since the main focus of the analysis is the Yukawa unification constraint on dark matter in SUGRA models⁴, we briefly discuss some broad features of this constraint with details to follow later. In the supersymmetric framework the unification of the Yukawa couplings of the third generation, as predicted in several grand unification models, is rather sensitive to the parameters of the SUSY models. Thus, the compatibility of $b - \tau$ unification at the

²There is also revived interest in the possibility that the LSP in SUGRA models could be the gravitino. For an update see Ref.[5]

³For an analysis of dark matter with CP phases but without inclusion of the Yukawa unification constraints see Refs.[6, 7]. An analysis of dark matter with quasi Yukawa unification was given in Refs.[8, 9].

⁴For recent works on dark matter analyses in SUGRA models see Ref.[10]

grand unification scale with the observed b and τ masses depends sensitively on the sign of μ^5 (where μ is the Higgs mixing parameter) as well as on the details of the sparticle spectrum [12, 13]. Moreover, for most of the available parameter space b - τ unification is in conflict with other experimental constraints such as the FCNC process $b \rightarrow s\gamma$. The more stringent $b - t - \tau$ unification is predicted in the minimal $SO(10)$ models where the quarks and leptons, residing in the 16-plet spinor representation of $SO(10)$, gain masses via coupling with a 10-plet tensor representation of $SO(10)$ ⁶ [14, 15, 16, 17]. Finally, we mention that there can be GUT scale threshold corrections to the Yukawa unification. However, typically they are expected to be small [18].

Let us now be more specific and review the situation of Yukawa coupling unification in the mSUGRA case with no phases. With universal Yukawa couplings at the grand unification scale, the masses of the bottom and the top quark are naturally higher than the τ lepton mass. This phenomenon arises because of the color interactions which causes the Yukawa couplings of the quarks to increase as one goes down to lower energy scales. Thus, the running quark masses end up larger than the running charged lepton masses. To convert the running mass to the pole mass, one needs to include the supersymmetric as well as the standard model (SM) threshold corrections. In particular, it is well known that the supersymmetric threshold correction to the bottom quark mass, Δm_b , can be very large. The value of Δm_b is enhanced for large values of $\tan\beta$, where $\tan\beta$ is the ratio $\langle H_u \rangle / \langle H_d \rangle$ and where H_u gives mass to the up quark and H_d gives mass to the down quark and the lepton. In the mSUGRA case with no CP phases, Δm_b takes the sign of μ [15] (unless the trilinear terms are very large). A negative SUSY threshold correction to m_b is required in models with $b - \tau$ unification, in order to obtain a b -quark mass in the allowed range. Therefore, b - τ unification points toward a negative value of the μ -parameter. However, a negative μ parameter makes the SUSY contribution to $\text{BR}(b \rightarrow s\gamma)$ positive and hence it adds to the SM contribution and the charged Higgs contribution. As a result, a heavy spectrum is required in order not to exceed the upper bound for this branching ratio.

The SUSY contribution to the muon anomalous magnetic moment also takes the sign of μ in mSUGRA [19], and more generally this contribution depends on CP phases [20].

⁵We use the sign convention on μ as in Ref.[11].

⁶More Higgs multiplets are needed to break the gauge symmetry correctly down to the standard model gauge symmetry, but typically these additional Higgs fields do not have couplings to quarks and leptons.

However, experimentally the situation is less clear regarding the implications of the $g_\mu - 2$ data. Thus, while the BNL experiment has significantly improved the accuracy of the $g_\mu - 2$ measurement [21], ambiguities in the hadronic error, which is needed to compute the deviation of the observed value from the Standard Model prediction, still persist. Currently, the largest source of error in the computation of the Standard Model prediction is the $O(\alpha^2)$ hadronic vacuum polarization correction. The most recent evaluation of this correction are done by (i) Davier et.al.[22] using the τ decay data, and by (ii) Hagiwara et.al.[23] using the low energy data from $e^+e^- \rightarrow$ hadrons. Assuming that the entire difference Δa_μ (where a_μ is defined so that the effective operator is $a_\mu(e/2m_\mu)\bar{\mu}\sigma_{\alpha\beta}\mu F^{\alpha\beta}$) between experiment and theory comes from supersymmetry, one finds that the supersymmetric contribution for the case of Davier et.al. is $(7.6 \pm 9.0) \times 10^{-10}$, while for the case of Hagiwara et.al., the value is $(23.9 \pm 10.0) \times 10^{-10}$. In this analysis we adopt solution (i). In fact, in most of the parameter space we explore the sparticle spectrum is rather heavy, and the SUSY contribution Δa_μ small, and thus the a_μ prediction is essentially the same as the Standard Model prediction which is consistent with the current data. Solution (ii) puts a more stringent constraint. However, the constraint can be softened if the universality condition on the soft terms is removed [24, 25, 26].

As indicated earlier this paper is devoted mostly to an analysis of the WMAP data with the $b-\tau$ unification constraint. However, we will also briefly discuss $b-\tau-t$ unification. As is well known such a unification requires large $\tan\beta$ and for this reason much of the parameter space is excluded since it does not correctly break the electro-weak symmetry. Several studies has been done, and models such as, e.g., the D-term splitting in $SO(10)$ or non-universal Higgs masses can indeed give rise to a viable $t-b-\tau$ unification [27, 28, 29, 30, 31]. However, typically these solutions require a very heavy SUSY spectrum. Thus, the predicted dark matter abundance of neutralinos, in models with R-parity conservation, will be too high and thus will over-close the universe. As mentioned earlier, models with quasi unification have also been investigated [8, 9].

In the present work we first analyze the relic density within mSUGRA and show that there exist regions of the parameter space where the WMAP relic density constraint, the Yukawa unification constraint, and the $BR(b \rightarrow s\gamma)$ constraint can all be simultaneously satisfied. We then extend the mSUGRA parameter space retaining universality on the magnitude of the soft parameters but allowing non-universality for the phases in some sectors. The SUSY contribution to Δm_b is phase-dependent [32, 6] and this allows one to

determine the phases in some cases such as to obtain $m_b(M_Z)$ in the experimental range and thus achieve b - τ unification. Indeed, one finds that with the inclusion of phases $b - \tau$ unification is achievable in a large area of the parameter-space. Further, it is possible to find arrangement of phases such that the prediction of the electric dipole moments (EDMs) is in agreement with the experimental bounds. The case of full Yukawa unification is, however, still (almost) incompatible with the experimental value for $\text{BR}(b \rightarrow s\gamma)$. However, it is worth keeping in mind that small flavor mixings in the sfermion mass matrices can substantially change the predictions for $\text{BR}(b \rightarrow s\gamma)$ while leaving other predictions essentially untouched. Thus, in principle, non-zero CP-phases could also allow viable b - τ - t unification modulo mixings in the squark flavor sector. However, we do not pursue this line of investigation in the work here.

The outline of the rest of the paper is as follows: In Sec.(2) we give a discussion of the parameter space of the model and the details of the procedure of the calculations. In Sec.(3) we discuss the calculation of the $\text{BR}(b \rightarrow s\gamma)$ and resolve some of the ambiguities present in the literature in the large $\tan\beta$ enhanced contributions, by carrying out an independent analysis of the parameters $\epsilon'_b(t), \epsilon'_t(s), \epsilon_{bb}$, which codify these contributions. In Sec.(4) we carry out an analysis of the relic density with the b - τ unification constraint, and with the $\text{BR}(b \rightarrow s\gamma)$ constraint both within mSUGRA and in extended SUGRA models with phases. In Sec.(5) we give an analysis of the relic density for the case of the full Yukawa unification. In Sec.(6) we discuss the consistency of the analysis with large phases with the EDM constraints and give examples of models with large phases consistent with the WMAP data, b - τ unification and with the EDM constraints. Conclusions are given in Sec.(7).

2 Constraints on SUGRA models with CP-phases

Within mSUGRA there are only two physical phases, which can be chosen as θ_μ , the phase of the Higgs mixing parameter μ , and α_0 the phase of the universal trilinear term A_0 . These phases are severely constrained by the non-observation of the electric dipole moments (EDM). The present upper bounds for the EDM of the electron, of the neutron, and of the mercury ^{199}Hg atom are [33, 34, 35]

$$|d_e| < 4.23 \times 10^{-27} \text{ e cm}, \quad |d_n| < 6.5 \times 10^{-26} \text{ e cm}, \quad C_{\text{Hg}} < 3.0 \times 10^{-26} \text{ cm}, \quad (2)$$

where C_{Hg} is defined as in Ref.[36]. Large phases can be accommodated in several scenarios such as models with heavy sfermions [37], models with the cancellation mechanism [38], models with phases only in the third generation [39], or models with a non-trivial soft flavor structure [40]. Here, we use the cancellation mechanism [38]⁷ which becomes possible if the SUGRA parameter space is extended to allow for different gaugino phases. The model we consider is thus described by the following parameters

$$m_0, m_{1/2}, \tan \beta, |A_0|, \theta_\mu, \alpha_0, \xi_1, \xi_2, \xi_3, \quad (3)$$

where, ξ_i is the phase of the gaugino mass $M_i, i = 1, 2, 3$. The value of $|\mu|$ is determined by imposing electroweak symmetry breaking (EWSB).

In the analysis we use a top-down approach, and thus impose Yukawa unification at the GUT scale, M_{GUT} . For $b - \tau$ unification we have two independent Yukawa couplings at the grand unification scale, i.e., one common h_{uni} for the b and the τ , and one for the top-quark. We use these to fit the experimental value of the τ and the top masses. Unless another value is specified, we fix the top mass at 178 GeV, which is its current experimental central value [42]. The value of α_s is fixed to be 0.1185. For the τ mass at the electroweak scale M_Z , we use 1.7463 GeV, which takes into account the Standard Model radiative correction. Naturally, we also take into account the SUSY correction, as derived in [32], when calculating m_τ . In the case of the full Yukawa unification we impose $h_b = h_t = h_\tau = h_{\text{uni}}$ at M_{GUT} . Therefore, the value of $\tan \beta$ is fixed, since the two parameters h_{uni} and $\tan \beta$ are varied so as to obtain agreement with experimental values of m_τ and m_{top} . As the b -quark couples to the same Higgs doublet (H_d) as the τ lepton, its mass is fixed by h_{uni} . Therefore, $m_b(M_Z)$ is a prediction of our model and we require its value to be within the 2σ range,

$$2.69 \text{ GeV} < m_b(M_Z) < 3.10 \text{ GeV} \quad (4)$$

as described in [8]. In addition to the above, the other important constraints of the analysis are the relic density and the $\text{BR}(b \rightarrow s\gamma)$ constraint (see section 3).

The procedure for the calculation of the particle and sparticle masses is as follows; After choosing a given set of the parameters in Eq.(3), we run the renormalization group equations (RGEs) down to the SUSY scale, defined as the average of the two stop masses.

⁷For a more complete list of references and for a discussion of the effects of CP phases on low energy processes see Ref.[41].

At the SUSY scale the scalar potential is minimized and $|\mu|$ is calculated along with the SUSY threshold corrections to, e.g., the b quark and the τ lepton masses and the couplings are corrected accordingly. Hereafter, the sparticles are decoupled and the SM RGEs are used to run down to M_Z . At the electro-weak scale we check if the gauge couplings, the Weinberg angle, the top quark and the τ lepton masses are in agreement with their experimental values. If not, the RGEs are run iteratively until convergence is achieved. In the analysis we use the two-loop SUSY renormalization group equations [43] except for the trilinear terms, the gaugino and sfermion masses, which are calculated at the one-loop level. The SUSY renormalization group equation will also be influenced by the CP-phases. However, it is easy to see that neither the phase of the μ -term nor the phases of the gaugino masses will run. But, the phases of the trilinear terms run, and in general there will be three different phases at the low energy scale namely, α_t , α_b and α_τ . α_t is important as it affects Δm_b as well as $\text{BR}(b \rightarrow s\gamma)$. However, its value is almost fixed by the gluino phase. As shown in Ref.[44], the approximate relation $A_{\text{top}} \propto -M_3$ holds at low energy.

The regions of the mSUGRA parameter space that allows for acceptable relic abundance can be classified as: (i) the $\chi - \tilde{\tau}$ coannihilation region, (ii) the resonance region, and (iii) the Hyperbolic Branch/Focus Point (HB/FP) region[45]. In a previous work [6], we pointed out the strong variation of Δm_b with CP phases. In that work we focussed on the effects induced by the SUSY corrections on the spectrum and their consequences for the neutralino relic density. It was shown that the CP-phases have a very large impact on the value of the CP-odd Higgs mass M_A , which in turn affects the predicted dark matter abundance in the so-called resonance region. The analysis of Ref.[6] used a bottom-up approach by fixing the value of $m_b(M_Z)$ to its central value. In this work we use a top-down approach and large effects of the CP phases are not seen. In fact, the predicted neutralino relic abundance, turns out almost independent of the phases in the resonance region. In the stau coannihilation region there is also very little dependence on the CP-phases, except for the trilinear phase. As we show below, the HB/FP region cannot give rise to Yukawa unification within our model. In the calculation of the relic density we take into account the CP even-CP odd Higgs mixing. In the MSSM, after spontaneous breaking of the electro-weak symmetry one has at the tree-level two CP even Higgs (h^0, H^0) and one CP odd Higgs (A). In the presence of CP violating phases these mix, producing mass

eigenstates (H_1^0, H_2^0, H_3^0) , which are no longer eigen-functions of CP [61]⁸

The most important supersymmetric threshold correction is the one to the bottom mass. At the loop level the effective b quark coupling with the Higgs is given by [46]

$$-\mathcal{L}_{bbH^0} = (h_b + \delta h_b) \bar{b}_R b_L H_1^0 + \Delta h_b \bar{b}_R b_L H_2^{0*} + H.c. \quad (5)$$

The correction to the b quark mass is then given directly in terms of Δh_b and δh_b by

$$\Delta m_b = [Re(\frac{\Delta h_b}{h_b}) \tan \beta + Re(\frac{\delta h_b}{h_b})]. \quad (6)$$

We use the full analysis of Δm_b derived in [32]. The largest contributions to Δm_b are the gluino and the chargino exchange contributions. The gluino exchange contribution is proportional to $M_3 \mu$, and will therefore depend on the phase combination $\theta_\mu + \xi_3$. The chargino exchange contribution is usually smaller, except for very large values of $|A_t|$, since it is proportional to $A_t \mu$. Its dominant phase dependence is given by $\theta_\mu + \alpha_t$, and it has the opposite sign of the gluino contribution in a large region of the parameter space. When evaluating h_b at M_{SUSY} , we take into account threshold corrections using the relation⁹

$$h_b^{\text{SM}} = h_b^{\text{SUSY}} (1 + \Delta m_b). \quad (7)$$

The SM Yukawa coupling is evolved down to the electroweak scale, and the bottom quark mass

$$m_b(M_Z) = h_b^{\text{SM}} \frac{v}{\sqrt{2}} \cos \beta, \quad (8)$$

is calculated and compared with experiment. Similar expressions hold for the τ lepton with b replaced by τ . For the top quark at the Z scale one has

$$m_t(M_Z) = \frac{v}{\sqrt{2}} \sin \beta h_t^{\text{SUSY}} (1 + \Delta m_t) \quad (9)$$

where

$$\Delta m_t = [Re(\frac{\Delta h_t}{h_t}) \cot \beta + Re(\frac{\delta h_t}{h_t})]. \quad (10)$$

A full analysis of Δm_t is given in Ref. [32]. However, in the region of interest which corresponds to large $\tan \beta$ the correction to the top quark Yukawa is essentially negligible.

⁸For further details regarding the implications of these CP even-CP odd Higgs mixings on neutralino dark matter analysis see Ref.[6].

⁹This relation resums the SUSY self-energy leading order logarithmic corrections [47].

3 BR($b \rightarrow s\gamma$) with CP-phases

The present average for the BR($b \rightarrow s\gamma$) derived from the available experimental data [49] is found to be,

$$\text{BR}(b \rightarrow s\gamma) = (3.54^{+0.30}_{-0.28}) \times 10^{-4}, \quad (11)$$

by the *Heavy Flavor Averaging Group* [48]. The error includes an uncertainty due to the decay spectrum as well as the statistical error. The theoretical SM prediction is [50, 51],

$$\text{BR}(b \rightarrow s\gamma) = (3.70 \pm 0.30) \times 10^{-4}. \quad (12)$$

The above result uses the \overline{MS} running charm mass instead of the pole mass. It was claimed in Ref. [50] that this consideration reduces the NNLO uncertainty in the SM calculation. However, other analyses [52, 53] question the theoretical precision of Eq.(12) predicting a lower central value for the SM result. In any case, the result of Eq.(12) appears to be a good benchmark value for the SM prediction to work with.

The dominant SUSY contributions from the charged Higgs exchange include the $\tan\beta$ enhanced NLO corrections, which contribute to the Wilson coefficients C_7 and C_8 (these are coefficients of the operators $O_7 = \frac{e}{16\pi^2} m_b (\bar{s}_L \sigma_{\mu\nu} b_R) F_{\mu\nu}$ and $O_8 = \frac{g_s}{16\pi^2} m_b (\bar{s}_L \sigma_{\mu\nu} T^a b_R) G_{\mu\nu}^a$). These contributions can be codified in $\epsilon'_b(t)$, $\epsilon'_t(b)$ and ϵ_{bb} which enter in the Lagrangian for effective interaction involving the charged Goldstone boson and the charged Higgs boson as follows

$$\begin{aligned} \mathcal{L} = & \frac{g}{\sqrt{2}M_W} G^+ \left\{ \sum_d m_t V_{td} \bar{t}_R d_L - \sum_u m_b V_{ub} \frac{1 + \epsilon'_b(u) \tan\beta}{1 + \epsilon_{bb}^* \tan\beta} \bar{u}_L b_R \right\} \\ & + \frac{g}{\sqrt{2}M_W} H^+ \left\{ \sum_d m_t V_{td} \bar{t}_R d_L \frac{1 + \epsilon'_t(d) \tan\beta}{\tan\beta} + \sum_u m_b V_{ub} \bar{u}_L b_R \frac{\tan\beta}{1 + \epsilon_{bb}^* \tan\beta} \right\} + H.c. \end{aligned} \quad (13)$$

where V_{ij} is the CKM mixing matrix. Evaluation of $\epsilon'_b(t)$, $\epsilon'_t(b)$, and ϵ_{bb} exist in the literature [54, 55], but there is some ambiguity concerning the signs of some of the terms among the above groups. To resolve this we carry out an independent analysis of these quantities for the same loop diagrams as in the previous works, including also their dependence on CP phases, which was taken into account only in one analysis previously. Our analysis is derived using the work of Ref.[56]. We find

$$\epsilon'_b(t) = - \sum_{i=1}^2 \sum_{j=1}^2 \frac{2\alpha_s}{3\pi} e^{i\xi_3} D_{b2j}^* D_{t1i} \left[\frac{m_t}{m_b} \cot\beta A_t D_{b1j} D_{t2i}^* + \mu D_{b2j} D_{t1i}^* + m_t \cot\beta D_{b2j} D_{t2i}^* \right]$$

$$\begin{aligned}
& + \frac{m_t^2}{m_b} \cot \beta D_{b1j} D_{t1i}^* - \frac{m_W^2}{m_b} \sin \beta \cos \beta D_{b1j} D_{t1i}^* \Big] \frac{1}{|m_{\tilde{g}}|} H\left(\frac{m_{\tilde{t}_i}^2}{|m_{\tilde{g}}|^2}, \frac{m_{\tilde{b}_j}^2}{|m_{\tilde{g}}|^2}\right) \\
& + 2 \sum_{k=1}^4 \sum_{i=1}^2 \sum_{j=1}^2 \left[\frac{m_t}{m_b} \cot \beta A_t D_{b1j} D_{t2i}^* + \mu D_{b2j} D_{t1i}^* + m_t \cot \beta D_{b2j} D_{t2i}^* \right. \\
& \left. + \frac{m_t^2}{m_b} \cot \beta D_{b1j} D_{t1i}^* - \frac{m_W^2}{m_b} \sin \beta \cos \beta D_{b1j} D_{t1i}^* \right] \\
& \times (\alpha_{bk}^* D_{b1j}^* - \gamma_{bk}^* D_{b2j}^*) (\beta_{tk} D_{t1i} + \alpha_{tk}^* D_{t2i}) \frac{1}{16\pi^2} \frac{1}{m_{\chi_k^0}} H\left(\frac{m_{\tilde{t}_i}^2}{m_{\chi_k^0}^2}, \frac{m_{\tilde{b}_j}^2}{m_{\chi_k^0}^2}\right)
\end{aligned} \tag{14}$$

In the above D_q is the matrix that diagonalizes the squark mass² matrix M_q^2 , i.e.,

$$D_q^\dagger M_q^2 D_q = \text{diag}(M_{\tilde{q}_1}^2, M_{\tilde{q}_2}^2) \tag{15}$$

and $H(a, b)$ is defined by

$$H(a, b) = \frac{a}{(1-a)(a-b)} \ln a + \frac{b}{(1-b)(b-a)} \ln b \tag{16}$$

where $\alpha_{bk}, \beta_{bk}, \gamma_{bk}$ for the b quark and the corresponding coefficients for the t quark are as defined in Ref.[56]. Similarly for $\epsilon'_t(s)$ we find

$$\begin{aligned}
\epsilon'_t(s) &= \sum_{i=1}^2 \sum_{j=1}^2 \frac{2\alpha_s}{3\pi} e^{-i\xi_3} D_{s1i}^* D_{t2j} \left[\frac{m_s}{m_t} \tan \beta A_s^* D_{s2i} D_{t1j}^* + \mu^* D_{s1i} D_{t2j}^* + m_s \tan \beta D_{s2i} D_{t2j}^* \right. \\
& + \frac{m_s^2}{m_t} \tan \beta D_{s1i} D_{t1j}^* - \frac{m_W^2}{m_t} \sin \beta \cos \beta D_{s1i} D_{t1j}^* \Big] \frac{1}{|m_{\tilde{g}}|} H\left(\frac{m_{\tilde{s}_i}^2}{|m_{\tilde{g}}|^2}, \frac{m_{\tilde{t}_j}^2}{|m_{\tilde{g}}|^2}\right) \\
& - 2 \sum_{k=1}^4 \sum_{i=1}^2 \sum_{j=1}^2 \left[\frac{m_s}{m_t} \tan \beta A_s^* D_{s2i} D_{t1j}^* + \mu^* D_{s1i} D_{t2j}^* + m_s \tan \beta D_{s2i} D_{t2j}^* \right. \\
& \left. + \frac{m_s^2}{m_t} \tan \beta D_{s1i} D_{t1j}^* - \frac{m_W^2}{m_t} \sin \beta \cos \beta D_{s1i} D_{t1j}^* \right] \\
& \times (\beta_{sk}^* D_{s1i}^* + \alpha_{sk} D_{s2i}^*) (\alpha_{tk} D_{t1j} - \gamma_{tk} D_{t2j}) \frac{1}{16\pi^2} \frac{1}{m_{\chi_k^0}} H\left(\frac{m_{\tilde{s}_i}^2}{m_{\chi_k^0}^2}, \frac{m_{\tilde{t}_j}^2}{m_{\chi_k^0}^2}\right)
\end{aligned} \tag{17}$$

Finally, our analysis of ϵ_{bb} gives

$$\begin{aligned}
\epsilon_{bb} &= - \sum_{i=1}^2 \sum_{j=1}^2 \frac{2\alpha_s}{3\pi} e^{-i\xi_3} D_{b1i}^* D_{b2j} \left[\frac{M_Z m_W}{m_b} \frac{\cos \beta}{\cos \theta_W} \left\{ \left(-\frac{1}{2} + \frac{1}{3} \sin^2 \theta_W\right) D_{b1i} D_{b1j}^* \right. \right. \\
& \left. \left. - \frac{1}{3} \sin^2 \theta_W D_{b2i} D_{b2j}^* \right\} \sin \beta + \mu^* D_{b1i} D_{b2j}^* \right] \frac{1}{|m_{\tilde{g}}|} H\left(\frac{m_{\tilde{b}_i}^2}{|m_{\tilde{g}}|^2}, \frac{m_{\tilde{b}_j}^2}{|m_{\tilde{g}}|^2}\right)
\end{aligned}$$

$$\begin{aligned}
& - \sum_{i=1}^2 \sum_{j=1}^2 \sum_{k=1}^2 g^2 \left[\frac{M_Z m_W}{m_b} \frac{\cos \beta}{\cos \theta_W} \left\{ \left(\frac{1}{2} - \frac{2}{3} \sin^2 \theta_W \right) D_{t1i} D_{t1j}^* + \frac{2}{3} \sin^2 \theta_W D_{t2i} D_{t2j}^* \right\} \sin \beta \right. \\
& \left. - \frac{m_t^2}{m_b} \cot \beta \{ D_{t1i} D_{t1j}^* + D_{t2i} D_{t2j}^* \} - \frac{m_t}{m_b} \cot \beta A_t^* D_{t2i} D_{t1j}^* \right] \quad (18)
\end{aligned}$$

$$\times (V_{k1}^* D_{t1i}^* - K_t V_{k2}^* D_{t2i}^*) (K_b U_{k2}^* D_{t1j}) \frac{1}{16\pi^2} \frac{1}{|m_{\tilde{\chi}_k^+}|} H\left(\frac{m_{\tilde{t}_i}^2}{|m_{\tilde{\chi}_k^+}|^2}, \frac{m_{\tilde{t}_j}^2}{|m_{\tilde{\chi}_k^+}|^2}\right) \quad (19)$$

The form factor $H(a, b)$ in the above equation can have $a = b$ and in this case it reads

$$H(a, a) = \frac{1}{(a-1)^2} [1 - a + \ln a] \quad (20)$$

Before proceeding further we give a brief comparison of these results with the results of the previous works. The analysis of $\epsilon'_b(t)$ may be compared to ϵ_{tb} of Ref.[57] in the limit of large $\tan \beta$ and small squark mixings. In this case the limit of the first two lines in Eq.(15) agrees with the result of Ref.[57]. However, the limit of the last three lines of Eq.(15) have an opposite sign to that of Ref.[57]. Here our analysis is in agreement with the result of Ref.[58].

Next we give a computation of $\epsilon'_t(s)$. Approximating Eq.(18) we find

$$\begin{aligned}
\epsilon'_t(s) = & \sum_{i=1}^2 \sum_{j=1}^2 \frac{2\alpha_s}{3\pi} e^{-i\xi_3} \mu^* |D_{s1i}|^2 |D_{t2j}|^2 \frac{1}{|m_{\tilde{g}}|} H\left(\frac{m_{\tilde{s}_i}^2}{|m_{\tilde{g}}|^2}, \frac{m_{\tilde{t}_j}^2}{|m_{\tilde{g}}|^2}\right) \\
& - \frac{h_s^2}{16\pi^2} \frac{A_s^*}{m_{\chi_k^0}} X_{3k} X_{4k} |D_{s2i}|^2 |D_{t1j}|^2 H\left(\frac{m_{\tilde{s}_i}^2}{|m_{\tilde{\chi}_k^+}|^2}, \frac{m_{\tilde{t}_j}^2}{|m_{\tilde{\chi}_k^+}|^2}\right) \quad (21)
\end{aligned}$$

The analysis of Ref.[57] computed only the first line of Eq.(21) and for this part we agree with their work when we take the large $\tan \beta$ limit and the limit of small mixing angles of our result. The work Ref.[54] gives results corresponding to Eq.(21). However, here we find that we have a disagreement with the sign of the second part of their Eq.(16).

Our analysis of ϵ_{bb} given by our Eq.(19) agrees with the analysis of Ref.[57] in the limit of large $\tan \beta$ and in the limit of small squark mixings and here there is a general agreement (taking account of typo corrections) among various groups in the limit of no CP phases. Our analysis like that of Ref.[57] takes into account the full dependence on CP phases. In the numerical analysis to be presented below, we have used the code provided by micrOMEGAs [58] in the CP conserving case. This code agrees with the codes used by other groups [59]. In the CP violating case we have combined the codes of Refs.[58, 60] with our own codes of the SUSY contributions with CP phases.

For the uncertainty in $\text{BR}(b \rightarrow s\gamma)$ we use a linear combination of the errors on Eqs. (11) and (12). At the $2\text{-}\sigma$ level one has

$$2.3 \times 10^{-4} < \text{BR}(b \rightarrow s\gamma) < 4.7 \times 10^{-4} . \quad (22)$$

The numerical analysis given below is controlled essentially by the upper bound in Eq.(22). In order to obtain the correct value of $m_b(m_Z)$ one needs the phase combination $\theta_\mu + \xi_3$ to be close to π ¹⁰. In this case the chargino contribution to the $\text{BR}(b \rightarrow s\gamma)$ is positive and therefore the lower bound is not reached for the values of the SUSY parameters in our study. We turn now to the details of the numerical analysis.

4 WMAP Dark Matter Constraints and $b-\tau$ Yukawa unification

It is useful to first summarize our results in the mSUGRA case, where all CP phases are either zero or π . The relation $h_b = h_\tau$ can be satisfied for a wide range of soft masses in the MSSM with real universal soft terms. To discuss the dependence of $m_b(M_Z)$ on $\tan\beta$ we consider two representative set of soft parameters: (i) $m_{\frac{1}{2}} = 800$ GeV, $A_0 = 0$, $m_0 = 300$ GeV, and (ii) $m_{\frac{1}{2}} = 800$ GeV, $A_0 = 0$, $m_0 = 600$ GeV. In Fig. (1) we study the $\mu > 0$ and $\mu < 0$ cases for each set. The lines corresponding to case (i) are interrupted when $m_{\tilde{\tau}} < m_\chi$, while for case (ii) large values of $\tan\beta$ are incompatible with EWSB. We include a reference line ignoring the SUSY threshold corrections (i.e., $\Delta m_b = 0$). Fig. (1) exhibits the well known phenomenon, that Δm_b is positive for μ positive and therefore the theoretical prediction for the b quark pole mass is too high, lying outside the experimental range. Thus b- τ unification does not occur in this case. When $\mu < 0$, on the other hand, Δm_b is negative and the theoretical prediction for the b quark mass can lie within the experimental range for values of $\tan\beta$ between roughly 25 and 45. A similar analysis of $m_b(M_Z)$ but as a function of m_0 is given in Fig.(2). Here we consider only the $\mu < 0$ case and find that the theoretical prediction of $m_b(M_Z)$ can lie within the corridor allowed by experiment for a range of m_0 values. However, one finds that for very high values of m_0 , i.e., for values above 5 TeV and beyond, a region which includes

¹⁰The phase combination is drawn to smaller values for large $\tan\beta$ and for the full Yukawa unification it ends up close to $\pi/2$.

the Hyperbolic Branch (HB)/Focus Point (FP) region, Yukawa unification is not achieved with universal soft parameters.

We extend the analysis now to include the relic density constraints. Fig.(3) shows an area plot in the $m_0 - m_{\frac{1}{2}}$ plane and all the three interesting dark matter regions in mSUGRA can be seen. In Fig.(3) the coannihilation area and the resonance area overlap. The HB/FP area, which is the region adjacent to the area with no EWSB ($\mu^2 < 0$), is incompatible with any kind of Yukawa unification within the framework of universality of soft parameters at the GUT scale as already seen in the analysis of Fig.(2).

The HB/FP region moves to lower values of m_0 as $\tan\beta$ and m_t decrease and this variation, especially with m_t , can be very large (we present our analysis in Figs.(2,3) using $m_t = 176$ GeV in order that the HB/FP area appear below 20 TeV). With m_t at its lower bound the HB/FP region appears at values of m_0 of 5-6 TeV, but here m_b is already too high. With large values of $\tan\beta$, m_A^2 becomes negative before μ becomes small and therefore there is no inversion of the gaugino/Higgsino components in the composition of χ^0 . Correspondingly, the HB/FB is not reached. This is the case for the line of $\tan\beta = 48$ in Fig.2. Therefore, overlapping of the HB/FP region and the allowed m_b area is not possible. Moreover, phases cannot improve the situation as Δm_b is very small in the HB/FP (below 5%), and thus cannot lower the value of m_b sufficiently.

In Fig. (4) we further analyze the mSUGRA case with area plots in the $m_0 - m_{\frac{1}{2}}$ plane for four values of $\tan\beta$: 30, 35, 40, 45. Fig. (4) shows that the relic abundance, $b - \tau$ unification, and $b \rightarrow s\gamma$ constraints can be simultaneously satisfied for a narrow range of parameters for values of $\tan\beta$ in the range 30–45. The $\text{BR}(b \rightarrow s\gamma)$ constraint is a major restriction, since both SUSY and Higgs contributions to the branching ratio add to the one from the Standard Model, and thus one needs a relatively heavy spectrum such that the $\text{BR}(b \rightarrow s\gamma)$ prediction remains below the experimental upper bound. The $b - \tau$ unification constraint and the WMAP constraint further reduce the parameter space. Even so, one finds that there exist regions of the parameter space for all the four cases in Fig. (4) consistent with the WMAP data under the $b - \tau$ unification and $b \rightarrow s\gamma$ constraints.

4.1 Effects of CP phases

To determine the impact of phases on the above picture we choose two representative points from Fig. 4:

$$a) \tan\beta = 30, m_0 = 290 \text{ GeV}, M_{1/2} = 800 \text{ GeV}, A_0 = 0 \text{ GeV} \quad (23)$$

$$b) \tan\beta = 40, m_0 = 710 \text{ GeV}, M_{1/2} = 800 \text{ GeV}, A_0 = 0 \text{ GeV} \quad (24)$$

These points are chosen because in the absence of phases the WMAP relic density constraints are satisfied by different mechanisms for these two cases. Thus, for the point in Eq.(23) the WMAP constraint is satisfied due to $\chi - \tilde{\tau}$ coannihilations. In contrast, for the point in Eq.(24) the WMAP constraint is satisfied due to a resonance in the Higgs mediated annihilation of $\chi - \chi$. To determine the effect of phases we study the most relevant phases for the processes that we consider. The phases ξ_1 and ξ_2 have little impact on $b \rightarrow s\gamma$ and Δm_b . For simplicity we set them to zero in this section. We have already discussed the phase combinations that play an important role in the analysis of Δm_b . For the analysis of $b \rightarrow s\gamma$ we find that the same phase combinations, i.e, $Arg(\mu A_t)$ and $Arg(\mu M_3)$ are the important ones.

We now discuss the specifics of the point in Eq. (23), which as already stated is in the $\chi - \tilde{\tau}$ coannihilation region. In Fig.(5) we analyze the $BR(b \rightarrow s\gamma)$ and the $b - \tau$ unification constraints in the $\theta_\mu - \xi_3$ plane, and as is seen the point satisfies the $b \rightarrow s\gamma$ as well as $m_b(M_Z)$ constraint in the mSUGRA case with a negative μ . The figure illustrates that the inclusion of phases changes the value of $m_b(M_Z)$ and $BR(b \rightarrow s\gamma)$ drastically. However, the two above mentioned constraints have a tendency to conflict with each other, even with the inclusion of CP phases. Nevertheless, we find that there exists a substantial overlap of the areas allowed by the bounds on $m_b(M_Z)$ and $BR(b \rightarrow s\gamma)$. At the same time the predicted $\Omega_{CDM}h^2$ remains inside the WMAP bounds because the phases do not affect significantly the ratio $m_\chi/m_{\tilde{\tau}}$ and hence the relic density prediction remains dominated by coannihilations. It is also instructive to study the effects of α_0 . In Fig. (6) we analyze the dependence on $|A_0|$ and α_0 for the point $\xi_3 = 0.3$ rad and $\theta_\mu = 2.4$ rad of Fig.(5). In the analysis of Fig. (6) the ratio $m_{\tilde{\tau}}/m_\chi$ does not exceed 1.08, and thus we remain in the coannihilation region allowing for the satisfaction of the relic density constraints. Furthermore, it is also possible to satisfy $BR(b \rightarrow s\gamma)$ and m_b bounds simultaneously for a wide range of $|A_0|$ and α_0 .

Next we analyze the implication of phases for the point in Eq. (24). As already indicated this point is within the resonance region in the mSUGRA case. However, the point produces a value for the $\text{BR}(b \rightarrow s\gamma)$ outside the experimental bounds as may be seen from Fig. (4). The effect of varying ξ_3 and θ_μ is analyzed in Fig. (7). Here one finds a substantial overlap of the areas allowed by the bounds on $m_b(M_Z)$ and $\text{BR}(b \rightarrow s\gamma)$ while the relic density prediction remains within the WMAP bounds. As already stated, this analysis is substantially different from the one given in Ref. [6] at $\tan\beta = 40$. There $m_b(M_Z)$ was fixed and the dependence of Δm_b on the phases has a big effect on the resonant channels. For the present case, the bottom Yukawa has only a small fluctuation due to the unification condition at the GUT scale. Thus its effect on the Higgs mass parameters through the RGE's is not as large as the one found in the analysis of Ref. [6]. Thus in the analysis of Ref. [6] no unification condition was assumed for the Yukawa couplings, and the only requirement on them was to predict fixed values for the fermion masses. In the case of m_b , the effects induced by the phases via Δm_b were compensated by variations on h_b so as to obtain a fixed $m_b(M_Z)$. Since such adjustments of h_b induced large changes on the Higgs parameters, the relic density was very sensitive to the phases. In the present case, h_b is approximately fixed by the condition $h_b = h_\tau$ at the GUT scale (where h_τ is determined by $\tan\beta$ and m_τ).

The fluctuation of Δm_b with the phases enters in the prediction of $m_b(M_Z)$ which is allowed to vary in its experimental range. Thus in contrast to the analysis of Ref. [6] h_b is not adjusted as the phases vary in the present analysis. The value of h_b is approximately fixed by the condition $h_b = h_\tau$ at the GUT scale. Consequently, the phases do not have a big effect on the Ωh^2 prediction in the present scenario. For example, in Fig. (7), Ωh^2 varies only in the approximate range 0.10 – 0.13. The effects of variations with α_0 for the point Eq. (24) are analyzed in Fig. (8). Specifically, Fig. (8) gives an analysis of the neutralino relic density in the $|A|_0 - \alpha_0$ plane for the input of Eq. (24) along with $\theta_\mu = .5$, $\xi_3 = 1.7$. One finds a considerable structure here exhibiting the important effects of α_0 in this case. The relic density remains within the WMAP bounds, in the dark hatched area, while the area above the dashed line has a relic density below the lower bound.

5 WMAP dark matter constraint and full Yukawa unification

In the above we discussed the satisfaction of the WMAP relic density constraints consistent with the $\text{BR}(b \rightarrow s + \gamma)$ and $b - \tau$ unification constraints within mSUGRA and its extensions including phases. It was seen that the loop corrections to the b quark mass (and to the τ lepton mass) play an important role in accomplishing $b - \tau$ Yukawa unification at the GUT scale consistent with the experimental values for the τ lepton and the b quark masses. The values of $\tan \beta$ used in the analysis above were fairly large, lying in the range up to 40 – 45. When $\tan \beta$ exceeds these values the possibility that full Yukawa unification for the third generation holds becomes feasible. Here we investigate this possibility in further detail to determine if WMAP relic density and the $\text{BR}(b \rightarrow s + \gamma)$ constraints can also be simultaneously satisfied. In the analysis we will allow for the dependence on CP phases.

In Fig. (9) we present an analysis of full Yukawa unification and we also display the constraints of relic density and of $\text{BR}(b \rightarrow s + \gamma)$. We impose full Yukawa unification at the GUT scale, the value of $\tan \beta$ is therefore fixed by the experimental τ and top masses. As before, $m_b(M_Z)$ is a prediction. Typically, there are two main constraints on m_0 and $m_{1/2}$ for a given A_0 . These are the condition of radiative EWSB (or almost equivalently $m_A < 120$ GeV) and the condition that the LSP be neutral. The constraints on m_0 and $m_{1/2}$ such that both conditions are met were described in an early paper [14] and also emphasized in Ref.[62] which gave the relation

$$m_A^2 = \alpha m_{1/2}^2 - \beta m_0^2 - \text{constant} \quad (25)$$

where the coefficients α and β are positive and ~ 0.1 , and the constant is $\sim M_Z$. Thus for fixed m_A one has a hyperbolic branch. Furthermore, the requirement that LSP be neutral, i.e. $m_\chi < m_{\tilde{\tau}}$, makes another cut in the allowed area. While Fig. (9) exhibits a narrow area where the WMAP relic density constraint is satisfied, one finds that $m_b(M_Z)$ is outside the experimental bounds (the line $m_b(M_Z) = 2.50$ GeV is presented as a reference line in Fig. (9)).

In the whole figure the value of $m_b(M_Z)$ lies below the lower experimental bound. The region satisfying the $\text{BR}(b \rightarrow s\gamma)$ bounds is also exhibited in Fig. (9). The charged Higgs contribution is enhanced in this case due to the low values of its mass, m_{H^\pm} (lines

corresponding to the values $m_{H^+} = 300$ and 500 GeV are given as reference). Since the SUSY contribution is also positive the value of $\text{BR}(b \rightarrow s + \gamma)$ lies below its upper experimental limit only for the small region found at $m_{1/2} \sim 2900$ GeV. For the SM contribution we followed the considerations of [50] by using the \overline{MS} running charm mass, so that $\frac{m_c}{m_b} = 0.29$. In this case the central value of Eq. 12 for the SM prediction is obtained. However, as argued in Ref.[52, 53] the theoretical SM prediction is possibly lower. Thus as an illustration we also give an analysis using the pole mass ratio $\frac{m_c}{m_b} = 0.29$ which leads to a SM prediction of 3.33×10^{-4} .

We investigate now the implications of extending the parameter space by CP phases for a selected point in the coannihilation region. Fig. (10) shows the $\theta_\mu - \xi_3$ plane for $m_0 = 880$ GeV, $M_{1/2}=1500$ GeV and $A_0 = 0$. The value of $\tan\beta$ lies in the range $51 - 54.5$. The prediction for the relic density remains in the WMAP range, since the neutralino remains in the coannihilation area. The regions where $m_b(M_Z)$ and $\text{BR}(b \rightarrow s\gamma)$ lie inside the experimental bounds are shown. There is only a rather tiny region, roughly at $\theta_\mu = \pi/2$ and $\xi_3 = 0$, where the Yukawa unification constraints and the $\text{BR}(b \rightarrow s\gamma)$ are simultaneously satisfied. This area is affected by the uncertainty in the determination of the SM value for $\text{BR}(b \rightarrow s\gamma)$. The area is significantly enlarged when the ratio $\frac{m_c}{m_b} = 0.29$ is used in the $\text{BR}(b \rightarrow s\gamma)$ computation.

6 Consistency with the EDM constraints.

With inclusion of phases, one has to account for the satisfaction of the EDM constraints. In the following we demonstrate that, there exist regions in the parameter space, where the WMAP, the $b - \tau$ unification, the $\text{BR}(b \rightarrow s\gamma)$ as well as the EDM constraints are all satisfied when the phases are large. In Table 1 we define two points, one for $\tan\beta = 40$ and another for $\tan\beta = 45$ where all constraints are satisfied as shown in Table 2.

A more detailed exhibition of the value of $m_b(M_Z)$ and $\text{BR}(b \rightarrow s + \gamma)$ as θ_μ and ξ_3 varies is given in Figs. (11) and (12) while ξ_1, ξ_2 are set at the values given in Table 1. It was shown in Ref.[63], that if the EDM constraints are satisfied for a given point, there exists a scaling region, where $m_0, m_{1/2}, A_0$ scale by a common factor λ , in which the EDM constraints also are satisfied, for a reasonable range of λ around one. The allowed range of λ depends on other dynamical parameters. For Point (i) m_0 and $m_{1/2}$ are related by $m_0 = 0.832 \cdot m_{1/2}$ while for Point (ii) this relation becomes $m_0 = 1.80 \cdot m_{1/2}$. For

point (ii) the EDM constraints are satisfied down to $m_{1/2} \sim 750$ GeV. In Fig. (13) we display $\text{BR}(b \rightarrow s\gamma)$ and the neutralino relic density for the case of two points in Table 1. The analysis shows that $m_b(M_Z)$ remains inside its experimental range for the range of parameters shown in the figure. The qualitative behavior of the relic density in both cases can be understood by comparison with the corresponding cases in Fig. 4. For $\tan\beta = 40$ the line $m_0 = 0.832 \cdot m_{1/2}$ has a sizeable overlap with the WMAP area, whereas for $\tan\beta = 45$ the line $m_0 = 1.832 \cdot m_{1/2}$ intersects the WMAP area. The values of $m_b(M_Z)$ ranges from 2.80 to 2.86 GeV for the case (i) and from 2.84 to 2.96 GeV for case (ii).

Point	m_0	$m_{\frac{1}{2}}$	$ A_0 $	$\tan\beta$	θ_μ	α_A	ξ_1	ξ_2	ξ_3
(i)	1040	1250	0	40	2.9	0	1.0	0.15	0.5
(ii)	1980	1100	0	45	0.6	0	0.5	-0.6	1.6

Table 1: Values of the parameters for point (i) and point (ii).

Point	$ d_e $ e.cm	$ d_n $ e.cm	C_{Hg} cm	Ωh^2	$\text{BR}(b \rightarrow s\gamma)$	$m_b(M_Z)$
(i)	1.33×10^{-27}	8.87×10^{-27}	1.72×10^{-26}	0.099	4.44×10^{-4}	2.85
(ii)	1.87×10^{-28}	2.71×10^{-26}	1.13×10^{-26}	0.112	4.37×10^{-4}	2.92

Table 2: The EDMs, the relic abundance Ωh^2 , the branching ratio $\text{BR}(b \rightarrow s\gamma)$, and the $m_b(M_Z)$ prediction for point (i) and point (ii) as defined in Table 1.

7 Conclusions

The main focus of this work is an analysis of the neutralino relic density consistent with the WMAP data under the constraint of $b - \tau$ Yukawa unification, and the constraint of $b \rightarrow s + \gamma$ branching ratio. In the analysis of the $b \rightarrow s + \gamma$ branching ratio, we have included the $\tan\beta$ enhanced NLO corrections which contribute to the Wilson coefficients. These enhancements are codified via the epsilon terms defined in Eq.(13). There is ambiguity in the sign of some of the terms among the various groups. To resolve this we carried out an independent calculation of these quantities as discussed in Sec.3. The analysis is carried out within SUGRA unified models where universality on

the magnitudes of soft parameters at the GUT scale is assumed, but we allow for CP violating phases and specifically allow non-universality of the phases in the gaugino mass sector. First we give an analysis for the case when all the soft parameters are real. This is the mSUGRA case, and here we find that for values of $\tan\beta$ in the range 27-48, one obtains an amount of dark matter consistent with WMAP as well as consistency with $b-\tau$ unification and with the $b \rightarrow s + \gamma$ constraint. An interesting phenomenon that arises is the following: There are three regions in the $m_0 - m_{\frac{1}{2}}$ parameter space where relic density and the $b \rightarrow s + \gamma$ constraint can be satisfied in general. These consist of the coannihilation region, the resonance region, and the HB/FP region. Of these only the first two can satisfy the Yukawa unification constraint. Thus the constraint of Yukawa unification narrows the available parameter space by eliminating the HB/FP region. We then extend this analysis to include phases and show that new regions of the parameter space allow for consistency with the WMAP data and other constraints extending the allowed region of the parameter space. In $b-\tau$ unification case we find explicit phase arrangements such that the EDM bounds are satisfied, $m_b(M_Z)$ and the rate for $\text{BR}(b \rightarrow s\gamma)$ lie within their experimental ranges, and the prediction of the neutralino relic density lies within the WMAP bounds. We have also given an analysis of the full $b - \tau - t$ Yukawa unification constraint with inclusion of CP phases. We find a small area where m_b is predicted inside the experimental range and the $\text{BR}(b \rightarrow s\gamma)$ bound is satisfied. Furthermore, the relic density of neutralinos lies within the WMAP bounds due to $\chi - \tilde{\tau}$ coannihilations. However, this area is rather small and moreover we could not find phase arrangements satisfying the EDM constraints. It is conjectured that inclusion of additional non-universalities could rectify the situation.

Acknowledgments

MEG acknowledges support from the 'Consejería de Educación de la Junta de Andalucía', the Spanish DGICYT under contract BFM2003-01266 and European Network for Theoretical Astroparticle Physics (ENTApP), member of ILIAS, EC contract number RII-CT-2004-506222. The research of TI and PN was supported in part by NSF grant PHY-0139967. PN also acknowledges support from the Alexander von Humboldt Foundation and thanks the Max Planck Institute, Munich for hospitality extended him. SS is supported by Fundação de Amparo à Pesquisa do Estado de São Paulo (FAPESP).

References

- [1] C. L. Bennett *et al.*, *Astrophys. J. Suppl.* **148**, 1 (2003) [arXiv:astro-ph/0302207].
- [2] D. N. Spergel *et al.* [WMAP Collaboration], *Astrophys. J. Suppl.* **148**, 175 (2003) [arXiv:astro-ph/0302209].
- [3] A.H. Chamseddine, R. Arnowitt and P. Nath, *Phys. Rev. Lett.* **49**, 970 (1982); R. Barbieri, S. Ferrara and C.A. Savoy, *Phys. Lett. B* **119**, 343 (1982); P. Nath, R. Arnowitt and A.H. Chamseddine, *Nucl. Phys. B* **227**, 121 (1983); L. Hall, J. Lykken, and S. Weinberg, *Phys. Rev. D* **27**, 2359 (1983). For a recent review see, P. Nath, “Twenty years of SUGRA,” arXiv:hep-ph/0307123.
- [4] H. Goldberg, *Phys. Rev. Lett.* **50**, 1419 (1983); J. R. Ellis, J. S. Hagelin, D. V. Nanopoulos, K. A. Olive and M. Srednicki, *Nucl. Phys. B* **238**, 453 (1984)
- [5] J. R. Ellis, K. A. Olive, Y. Santoso and V. C. Spanos, *Phys. Lett. B* **588**, 7 (2004) [arXiv:hep-ph/0312262].
- [6] M. E. Gomez, T. Ibrahim, P. Nath and S. Skadhauge, *Phys. Rev. D* **70**, 035014 (2004) [arXiv:hep-ph/0404025].
- [7] U. Chattopadhyay, T. Ibrahim and P. Nath, *Phys. Rev.* **D60**, 063505 (1999); T. Falk, A. Ferstl and K. Olive, *Astropart. Phys.* **13**, 301 (2000) ; M. Argyrou, A. B. Lahanas, D. V. Nanopoulos and V. C. Spanos, *Phys. Rev. D* **70**, 095008 (2004) ; T. Nihei and M. Sasagawa, *Phys. Rev. D* **70**, 055011 (2004).
- [8] M. E. Gomez, G. Lazarides and C. Pallis, *Nucl. Phys. B* **638**, 165 (2002) [arXiv:hep-ph/0203131].
- [9] M. E. Gomez, G. Lazarides and C. Pallis, *Phys. Rev. D* **67**, 097701 (2003) [arXiv:hep-ph/0301064].
- [10] H. Baer, A. Mustafayev, E-K. Park, S. Profumo, arXiv:hep-ph/0505227; H.. Baer, A. Mustafayev, S. Profumo, A. Belyaev and X. Tata, arXiv:hep-ph/0504001; S. Baek, D. G. Cerdeno, Y. G. Kim, P. Ko and C. Munoz, arXiv:hep-ph/0505019; A. Djouadi, M. Drees and J. L. Kneur, arXiv:hep-ph/0504090; G. Belanger, F. Boudjema, A. Cottrant, A. Pukhov and A. Semenov, arXiv:hep-ph/0412309;

- R. Arnowitt, B. Dutta and B. Hu, Phys. Rev. D **68**, 075008 (2003) [arXiv:hep-ph/0307152].
- [11] [SUGRA Working Group Collaboration], “Report of the SUGRA working group for run II of the Tevatron,” arXiv:hep-ph/0003154.
- [12] W. de Boer, M. Huber, A. V. Gladyshev and D. I. Kazakov, Eur. Phys. J. C **20**, 689 (2001) [arXiv:hep-ph/0102163].
- [13] S. Komine and M. Yamaguchi, Phys. Rev. D **65**, 075013 (2002) [arXiv:hep-ph/0110032]. ; U. Chattopadhyay and P. Nath, Phys. Rev. D **65**, 075009 (2002) [arXiv:hep-ph/0110341].
- [14] B. Ananthanarayan, Q. Shafi and X. M. Wang, Phys. Rev. D **50**, 5980 (1994) [arXiv:hep-ph/9311225].
- [15] L. J. Hall, R. Rattazzi and U. Sarid, Phys. Rev. D **50**, 7048 (1994) [arXiv:hep-ph/9306309]; M. Carena, M. Olechowski, S. Pokorski and C. E. Wagner, Nucl. Phys. B **426**, 269 (1994) [arXiv:hep-ph/9402253]; D. Pierce, J. Bagger, K. Matchev and R. Zhang, Nucl. Phys. **B491**, 3(1997).
- [16] H. Baer, M. A. Diaz, J. Ferrandis and X. Tata, Phys. Rev. D **61**, 111701 (2000) [arXiv:hep-ph/9907211].
- [17] H. Baer, M. Brhlik, M. A. Diaz, J. Ferrandis, P. Mercadante, P. Quintana and X. Tata, Phys. Rev. D **63**, 015007 (2001) [arXiv:hep-ph/0005027].
- [18] B. D. Wright, arXiv:hep-ph/9404217.
- [19] J. L. Lopez, D. V. Nanopoulos and X. Wang, Phys. Rev. D **49**, 366 (1994) [arXiv:hep-ph/9308336] ; U. Chattopadhyay and P. Nath, Phys. Rev. D **53**, 1648 (1996) [arXiv:hep-ph/9507386].
- [20] T. Ibrahim and P. Nath, Phys. Rev. D **62**, 015004 (2000) [arXiv:hep-ph/9908443] ; Phys. Rev. D **61**, 095008 (2000) [arXiv:hep-ph/9907555].
- [21] G. W. Bennett *et al.* [Muon g-2 Collaboration], Phys. Rev. Lett. **92**, 161802 (2004) [arXiv:hep-ex/0401008].

- [22] M. Davier, S. Eidelman, A. Hocker and Z. Zhang, Eur. Phys. J. C **31**, 503 (2003) [arXiv:hep-ph/0308213].
- [23] K. Hagiwara, A. D. Martin, D. Nomura and T. Teubner, Phys. Rev. D **69**, 093003 (2004) [arXiv:hep-ph/0312250].
- [24] U. Chattopadhyay, A. Corsetti and P. Nath, Phys. Rev. D **66**, 035003 (2002) [arXiv:hep-ph/0201001].
- [25] C. Pallis, Nucl. Phys. B **678**, 398 (2004) [arXiv:hep-ph/0304047].
- [26] S. Profumo, JHEP **0306**, 052 (2003) [arXiv:hep-ph/0306119].
- [27] R. Dermisek, S. Raby, L. Roszkowski and R. Ruiz De Austri, JHEP **0304**, 037 (2003) [arXiv:hep-ph/0304101].
- [28] C. Balazs and R. Dermisek, JHEP **0306**, 024 (2003) [arXiv:hep-ph/0303161].
- [29] D. Auto, H. Baer, C. Balazs, A. Belyaev, J. Ferrandis and X. Tata, JHEP **0306**, 023 (2003) [arXiv:hep-ph/0302155].
- [30] H. Baer, A. Belyaev, T. Krupovnickas and A. Mustafayev, JHEP **0406**, 044 (2004) [arXiv:hep-ph/0403214].
- [31] D. Auto, H. Baer, A. Belyaev and T. Krupovnickas, JHEP **0410**, 066 (2004) [arXiv:hep-ph/0407165].
- [32] T. Ibrahim and P. Nath, Phys. Rev. D **67**, 095003 (2003) [arXiv:hep-ph/0301110].
- [33] E. Commins, et. al., Phys. Rev. **A50**, 2960(1994).
- [34] P.G. Harris et.al., Phys. Rev. Lett. **82**, 904(1999).
- [35] S. K. Lamoreaux, J. P. Jacobs, B. R. Heckel, F. J. Raab and E. N. Fortson, Phys. Rev. Lett. **57**, 3125 (1986).
- [36] T. Falk, K.A. Olive, M. Prospelov, and R. Roiban, Nucl. Phys. **B560**, 3(1999); V. D. Barger, T. Falk, T. Han, J. Jiang, T. Li and T. Plehn, Phys. Rev. D **64**, 056007 (2001); T. Ibrahim and P. Nath, Phys. Rev. D **67**, 016005 (2003) arXiv:hep-ph/0208142.

- [37] P. Nath, Phys. Rev. Lett. **66** (1991) 2565 ; Y. Kizukuri and N. Oshimo, Phys. Rev. D **46**,3025(1992)
- [38] T. Ibrahim and P. Nath, Phys. Lett. B **418**, 98 (1998); Phys. Rev. D **57**, 478 (1998) ; T. Falk and K Olive, Phys. Lett. B **439**, 71(1998); M. Brhlik, G.J. Good, and G.L. Kane, Phys. Rev. D **59**, 115004 (1999).
- [39] D. Chang, W-Y.Keung, and A. Pilaftsis, Phys. Rev. Lett. **82**, 900(1999).
- [40] S. Abel, S. Khalil and O. Lebedev, Nucl. Phys. B **606**, 151 (2001); G. C. Branco *et al.*, Nucl. Phys. B **659**, 119 (2003).
- [41] T. Ibrahim and P. Nath, " Phases and CP violation in SUSY", Published in *Hamburg 2002, Supersymmetry and unification of fundamental interactions, vol. 1* 313-324, edited by P. Nath and P. Zerwas. e-Print Archive: hep-ph/0210251
- [42] DO Collaboration, Nature Vol.429, 638(June 2004).
- [43] S. P. Martin and M. T. Vaughn, Phys. Rev. D **50**, 2282 (1994) [arXiv:hep-ph/9311340].
- [44] M. Carena, M. Olechowski, S. Pokorski and C. E. M. Wagner, Nucl. Phys. B **426**, 269 (1994) [arXiv:hep-ph/9402253].
- [45] K.L. Chan, U. Chattopadhyay and P. Nath, *Phys. Rev. D* **58**, 096004 (1998); J. L. Feng, K. T. Matchev and T. Moroi, Phys. Rev. D **61**, 075005 (2000).
- [46] M. Carena and H. E. Haber, Prog. Part. Nucl. Phys. **50**, 63 (2003)
- [47] M. Carena, D. Garcia, U. Nierste and C. E. M. Wagner, Nucl. Phys. B **577**, 88 (2000) [arXiv:hep-ph/9912516].
- [48] <http://www.slac.stanford.edu/xorg/hfag>
- [49] R. Barate *et al.* [ALEPH Collaboration], Phys. Lett. B **429**, 169 (1998); S. Chen *et al.* [CLEO Collaboration], Phys. Rev. Lett. **87**, 251807 (2001) [arXiv:hep-ex/0108032]; P. Koppenburg *et al.* [Belle Collaboration], Phys. Rev. Lett. **93**, 061803 (2004) [arXiv:hep-ex/0403004]; K. Abe *et al.* [Belle Collaboration], Phys.

- Lett. B **511**, 151 (2001) [arXiv:hep-ex/0103042]; B. Aubert *et al.* [BABAR Collaboration], arXiv:hep-ex/0207074 and arXiv:hep-ex/0207076.
- [50] P. Gambino and M. Misiak, Nucl. Phys. B **611**, 338 (2001) [arXiv:hep-ph/0104034].
 - [51] A. J. Buras, A. Czarnecki, M. Misiak and J. Urban, Nucl. Phys. B **631**, 219 (2002) [arXiv:hep-ph/0203135].
 - [52] T. Hurth, E. Lunghi and W. Porod, Eur. Phys. J. C **33**, S382 (2004); Nucl. Phys. B **704**, 56 (2005).
 - [53] M. Neubert, arXiv:hep-ph/0408179.
 - [54] G. Degrossi, P. Gambino and G. F. Giudice, JHEP **0012**, 009 (2000) [arXiv:hep-ph/0009337].
 - [55] M. Carena, D. Garcia, U. Nierste and C. E. M. Wagner, Phys. Lett. B **499**, 141 (2001) [arXiv:hep-ph/0010003].
 - [56] T. Ibrahim and P. Nath, Phys. Rev. D **69**, 075001 (2004) [arXiv:hep-ph/0311242].
 - [57] D. A. Demir and K. A. Olive, Phys. Rev. D **65**, 034007 (2002) [arXiv:hep-ph/0107329].
 - [58] G. Belanger, F. Boudjema, A. Pukhov and A. Semenov, Comput. Phys. Commun. **149**, 103 (2002) [arXiv:hep-ph/0112278] and arXiv:hep-ph/0405253.
 - [59] J. R. Ellis, S. Heinemeyer, K. A. Olive and G. Weiglein, JHEP **0502**, 013 (2005) [arXiv:hep-ph/0411216].
 - [60] J. S. Lee, A. Pilaftsis, M. Carena, S. Y. Choi, M. Drees, J. R. Ellis and C. E. M. Wagner, Comput. Phys. Commun. **156**, 283 (2004) [arXiv:hep-ph/0307377].
 - [61] A. Pilaftsis, Phys. Rev. **D58**, 096010; A. Pilaftsis and C.E.M. Wagner, Nucl. Phys. **B553**, 3(1999); D.A. Demir, Phys. Rev. **D60**, 055006(1999); S. Y. Choi, M. Drees and J. S. Lee, Phys. Lett. B **481**, 57 (2000); T. Ibrahim and P. Nath, Phys. Rev. D **63**, 035009 (2001) ; T. Ibrahim, Phys. Rev. D **64**, 035009 (2001); T. Ibrahim and P. Nath, Phys. Rev. D **66**, 015005 (2002); S. W. Ham, S. K. Oh, E. J. Yoo,

C. M. Kim and D. Son, arXiv:hep-ph/0205244; M. Carena, J. R. Ellis, A. Pilaftsis and C. E. Wagner, Nucl. Phys. B **625**, 345 (2002).

[62] M. Olechowski and S. Pokorski, Nucl. Phys. B **404**, 590 (1993) [arXiv:hep-ph/9303274].

[63] T. Ibrahim and P. Nath, Phys. Rev. D **61**, 093004 (2000) [arXiv:hep-ph/9910553].

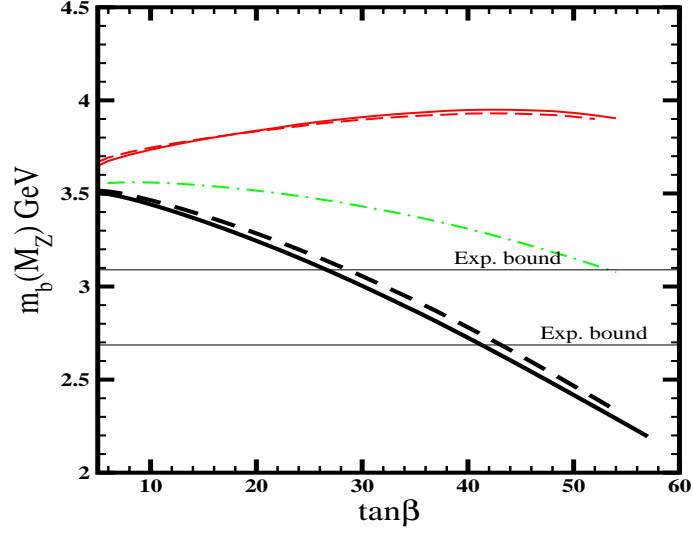


Figure 1: The value of $m_b(M_Z)$ versus $\tan \beta$ assuming $h_b = h_\tau$ at the GUT scale with $m_{1/2} = 800$ GeV, $A_0 = 0$ GeV, $m_0 = 300$ GeV (solid lines), $m_0 = 600$ GeV (dashed lines). The thick (thin) lines have $\mu < 0$ ($\mu > 0$). The dot-dashed line is plotted with $\Delta m_b = 0$.

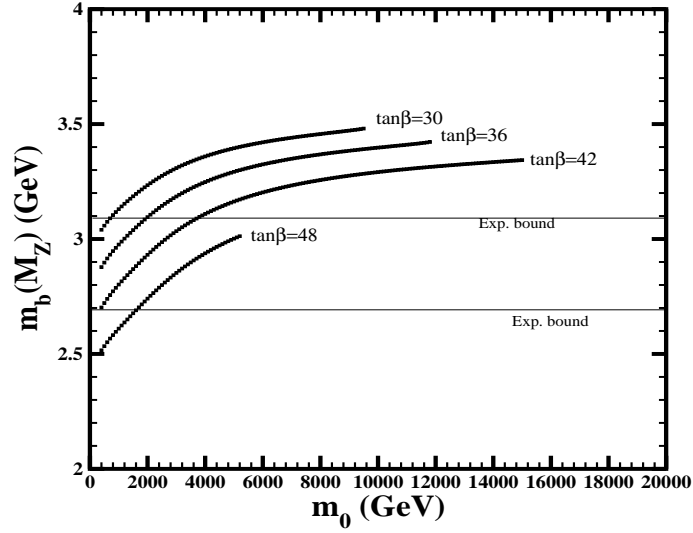


Figure 2: The value of $m_b(M_Z)$ using the constraint of $b - \tau$ Yukawa unification in mSUGRA. Furthermore, $m_t = 176$ GeV, $\mu < 0$ ($\theta_\mu = \pi$), $m_{1/2} = 800$ GeV, $A_0 = 0$ and the value of $\tan \beta$ has been varied as indicated on the curves. Lines ends at values of m_0 where EWSB is no longer satisfied, except for $\tan \beta = 48$, where the CP odd Higgs mass is too small.

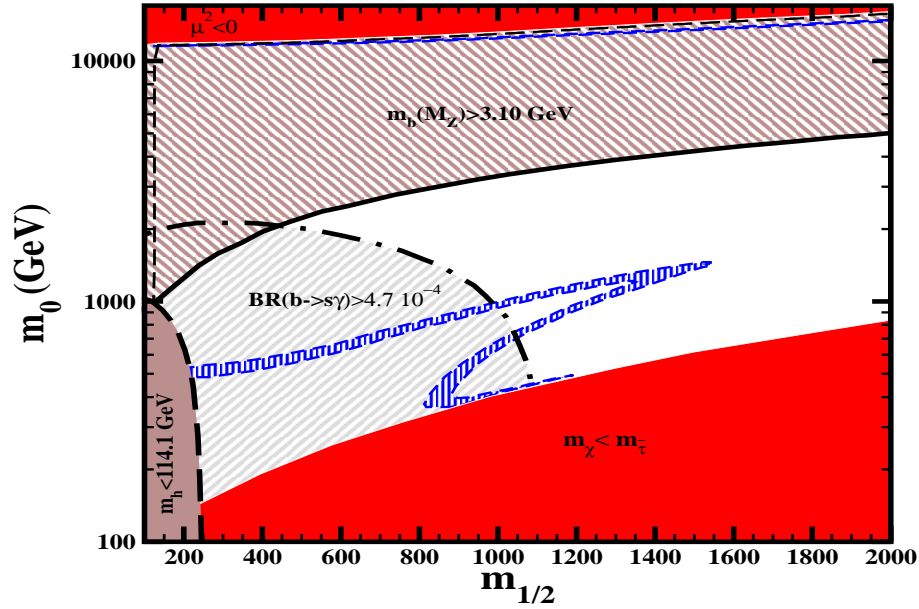


Figure 3: Analysis of neutralino relic density, $BR(b \rightarrow s\gamma)$ and of $m_b(M_Z)$ including the HB/FP region for $\tan\beta = 40$, $A_0 = 0$ and $m_t = 176$ GeV. Areas contoured by the dashed line has a neutralino relic density is inside the WMAP bounds. The area above the solid line predicts $m_b(M_Z) > 3.10$ GeV while the area inside the dashed (dot-dashed) line is excluded by the lower bound on m_h (the upper bound on $BR(b \rightarrow \gamma)$). On the lower dark shaded area $m_\chi > m_\tau$ while on the upper EWSB is not achieved. The thinner dashed line indicates $m_{\chi^+} = 103$ GeV.

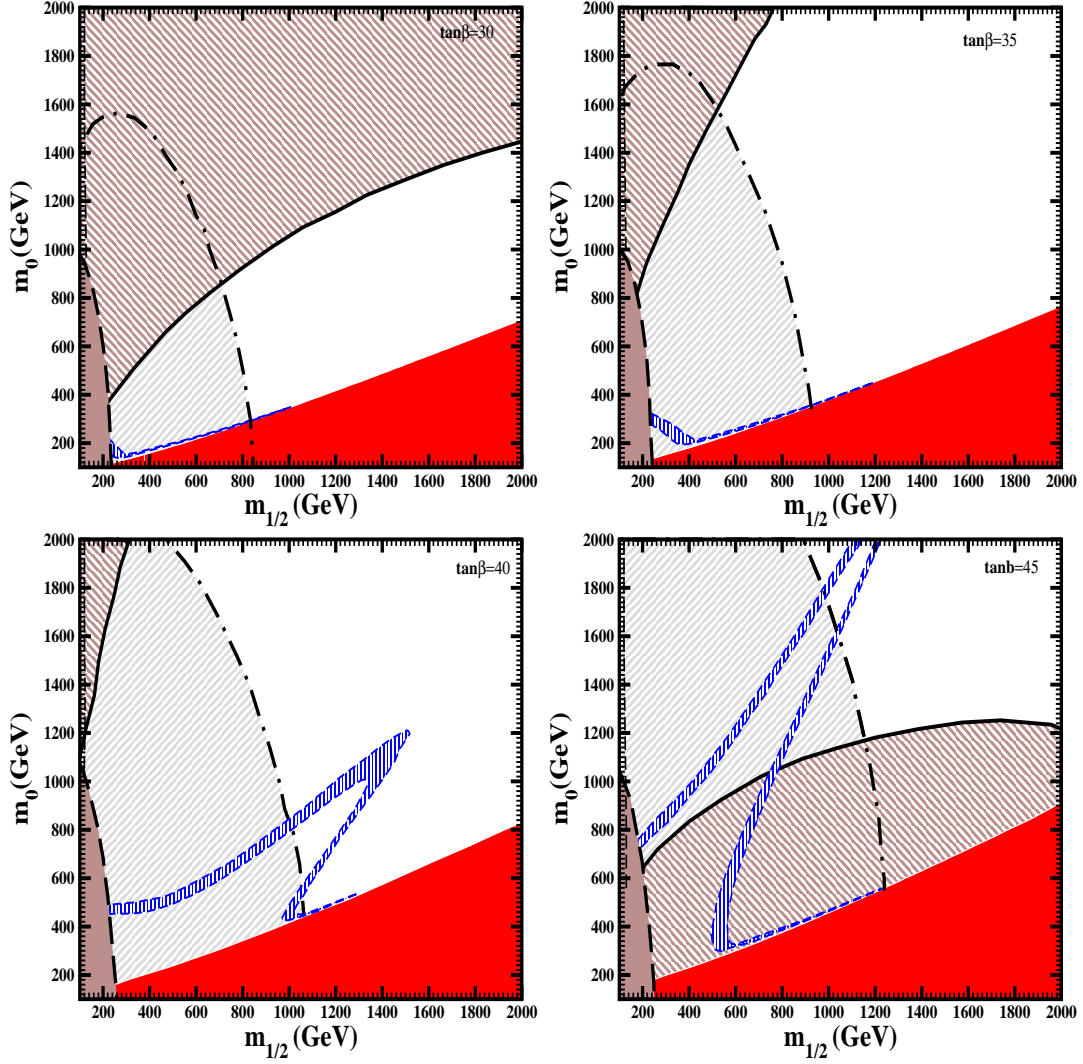


Figure 4: Analysis of the neutralino relic density with the $b - \tau$ Yukawa unification constraints in the $m_0 - M_{1/2}$ plane when the soft terms are universal and real with $\mu < 0$ ($\theta_\mu = \pi$), $A_0 = 0$, $m_t = 178$ GeV, and $\tan\beta = 30, 35, 40, 45$. The lines and shaded areas are as described in Fig.3. The area inside the solid line for the case $\tan\beta = 45$ predicts $m_b(M_Z) < 2.69$ GeV.

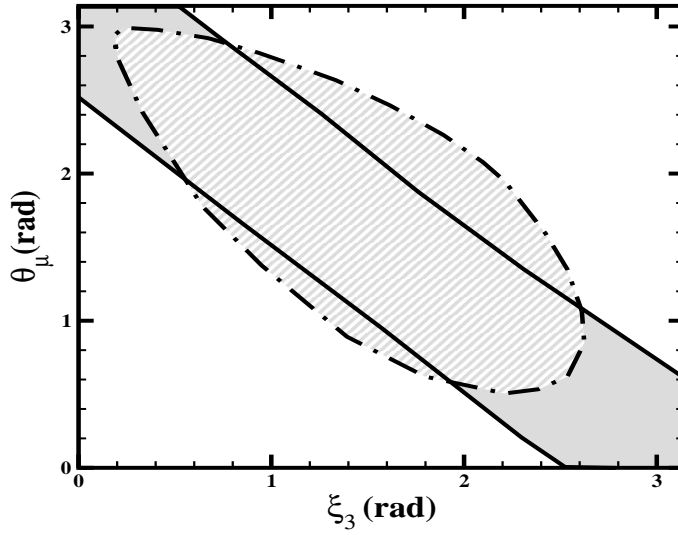


Figure 5: A plot in the $\xi_3 - \theta_\mu$ plane for $\tan\beta = 30$, $m_0 = 290$ GeV, $m_{1/2} = 800$ GeV, $A_0 = 0$ and $\xi_1 = \xi_2 = 0$. The area inside the solid lines predicts $m_b(M_Z)$ within the $2\text{-}\sigma$ experimental range. The area inside the dot-dashed line is excluded by the $\text{BR}(b \rightarrow s\gamma)$ constraint.

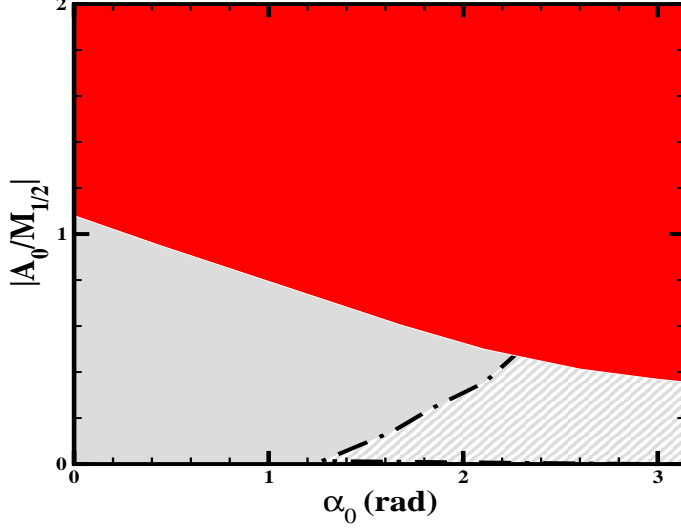


Figure 6: Analysis of $b - \tau$ unification in the $|A_0/m_{1/2}| - \alpha_0$ plane with phases corresponding to the point in Eq.(23) with $\xi_3 = 0.3$ rad, $\theta_\mu = 2.4$ rad and $\xi_1 = \xi_2 = 0$. In the dark shaded area, $m_\chi > m_{\tilde{\tau}}$ while within the ruled area bounded by the dot-dashed line $\text{BR}(b \rightarrow s\gamma)$ exceeds its upper limit. The grey area predicts $m_b(M_Z)$ inside the experimental bounds and fills the whole plane.

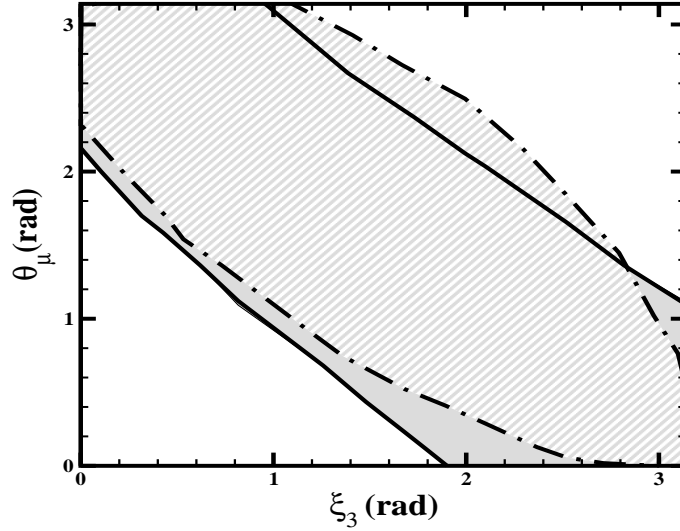


Figure 7: Same as Fig.5 except that $\tan\beta = 40$, $m_0 = 710$ GeV, $m_{1/2} = 800$ GeV, $A_0 = \xi_1 = \xi_2 = 0$

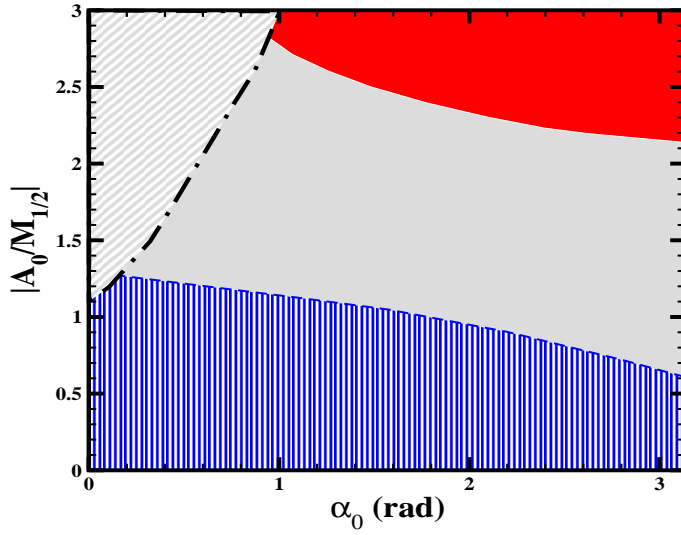


Figure 8: Analysis of the neutralino relic density in the $|A_0/m_{1/2}| - \alpha_0$ plane for $\xi_3 = 1.7$ rad, $\theta_\mu = 0.5$ rad while the other parameters are the same as in Fig.7. The area marking are the same as in Fig.6. The dark hatched area, contoured by the dashed, line predicts Ωh^2 inside the WMAP bounds.

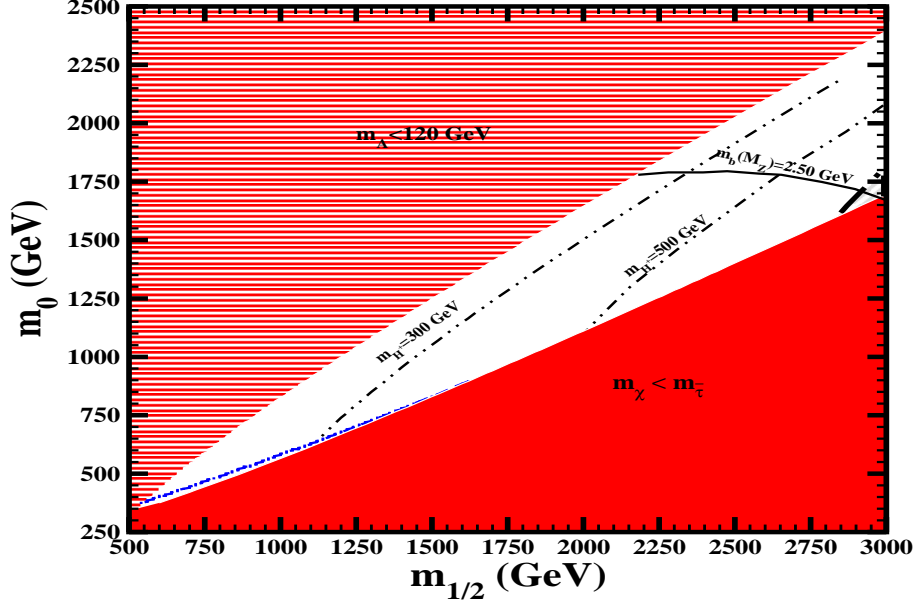


Figure 9: Analysis of the neutralino relic density, of $BR(b \rightarrow s + \gamma)$ and of $b - t - \tau$ unification in mSUGRA when $\mu < 0$ ($\theta_\mu = \pi$) and $A_0 = 0$. On the upper ruled area $m_A < 120$ GeV, while in the lower dark shaded area the lightest neutralino is not the LSP. The narrow area bounded by dash lines corresponds to the WMAP favored relic abundance prediction, while in the area, bounded by the dot-dashed thick line, the prediction for $BR(b \rightarrow s\gamma)$ is inside the experimental bounds. The thin dot-dashed line indicates the expansion of $BR(b \rightarrow s\gamma)$ allowed area when the ratio $\frac{m_c}{m_b} = 0.29$ is used in computation of the SM contribution. For the range of parameters exhibited, the prediction of $m_b(M_Z)$ is below the experimental bound, the solid line corresponds to a prediction of $m_b(M_Z) = 2.50$ GeV. The double-dotted-dashed line corresponds to the indicated values of m_{H^\pm} .

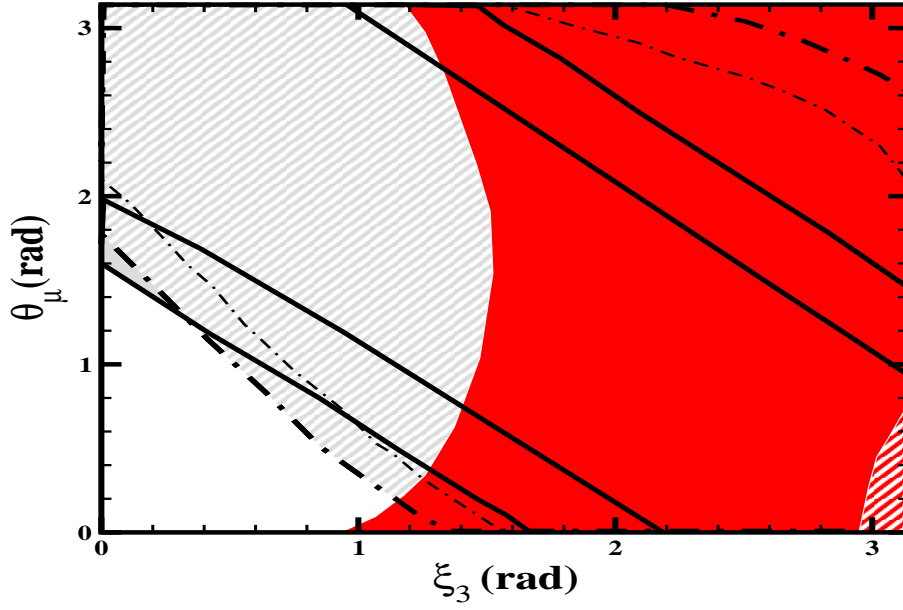


Figure 10: The full $b - t - \tau$ unification allowed areas (bounded by solid lines) and $\text{BR}(b \rightarrow s\gamma)$ excluded areas (bounded by dotted-dashed lines) in the $\theta_\mu - \xi_3$ plane, for $m_0 = 880$ GeV, $M_{1/2} = 1500$ GeV, $A_0 = 0$ GeV and all the remaining phases are set to zero. The area within the thin dotted-dashed line shows the expansion of the $b \rightarrow s\gamma$ allowed area when $\frac{m_c}{m_b} = 0.29$. In the dark shaded area the lightest neutralino is not the LSP, while in the dark hatched area in the right corner $m_A < 120$ GeV.

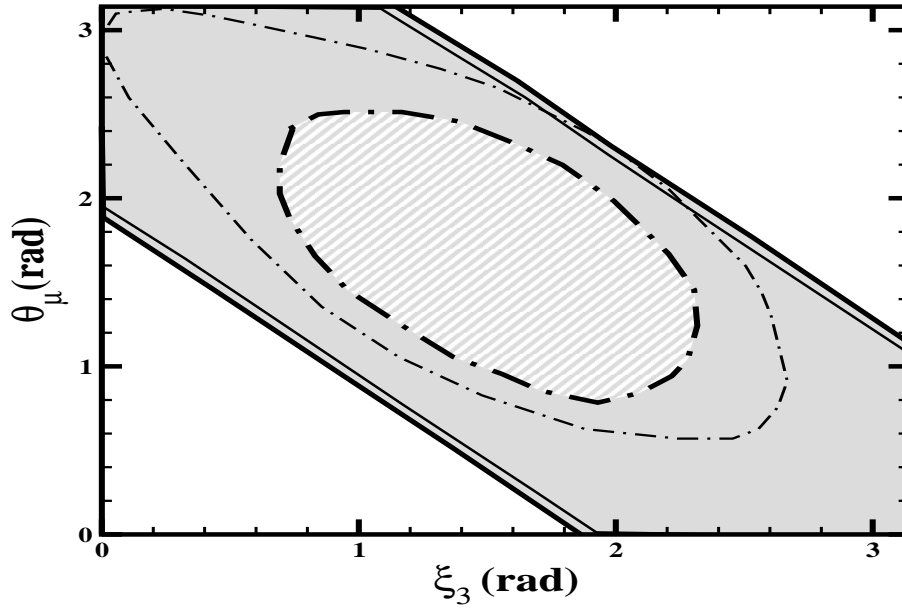


Figure 11: Analysis of the $b - \tau$ unification and the $\text{BR}(b \rightarrow s\gamma)$ constraints in the $\theta_\mu - \xi_3$ plane for $\tan\beta = 40$, $\xi_1 = 1.0$, $\xi_2 = 0.15$ and $A_0 = 0$. m_0 and $m_{1/2}$ satisfies $m_0 = 0.832 \cdot m_{1/2}$. In the area contoured by solid lines m_b is inside the experimental range, while the area inside the dotted-dashed line is excluded by the $\text{BR}(b \rightarrow s\gamma)$ bound. The thicker (thinner) lines correspond to $m_{1/2} = 1250$ GeV (1050 GeV).

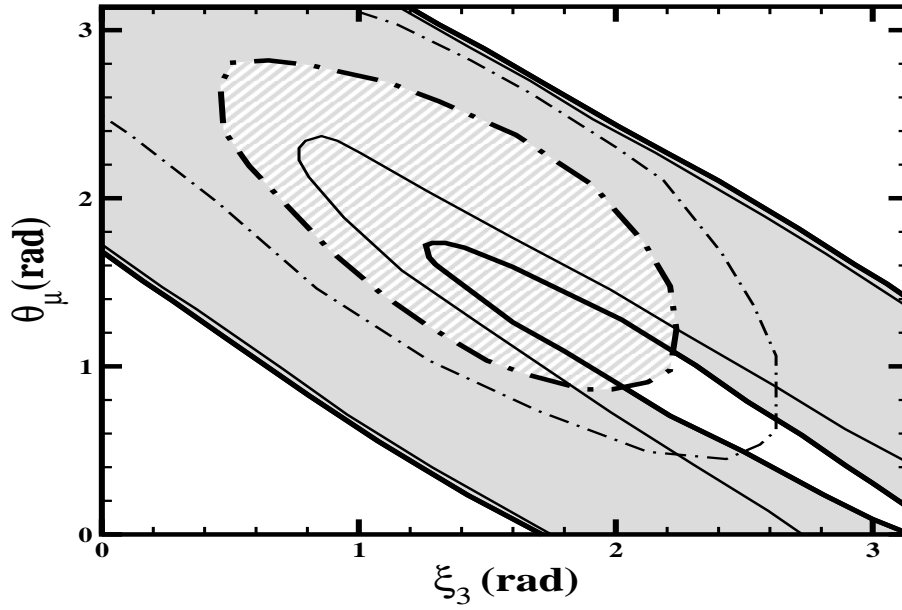


Figure 12: Analysis of $b - \tau$ unification and of $\text{BR}(b \rightarrow s\gamma)$ in the $\theta_\mu - \xi_3$ plane for $\tan\beta = 45$, $\xi_1 = 0.5$, $\xi_2 = -0.6$ and $A_0 = 0$. m_0 and $m_{1/2}$ satisfies the equation $m_0 = 1.8 \cdot m_{1/2}$. In the area contoured by solid lines m_b is inside the experimental bounds, while the area inside the dot-dash line is excluded by the higher($\text{BR}(b \rightarrow s\gamma)$) bound. The thicker (thinner) lines correspond to $m_{1/2} = 1000$ GeV (800 GeV).

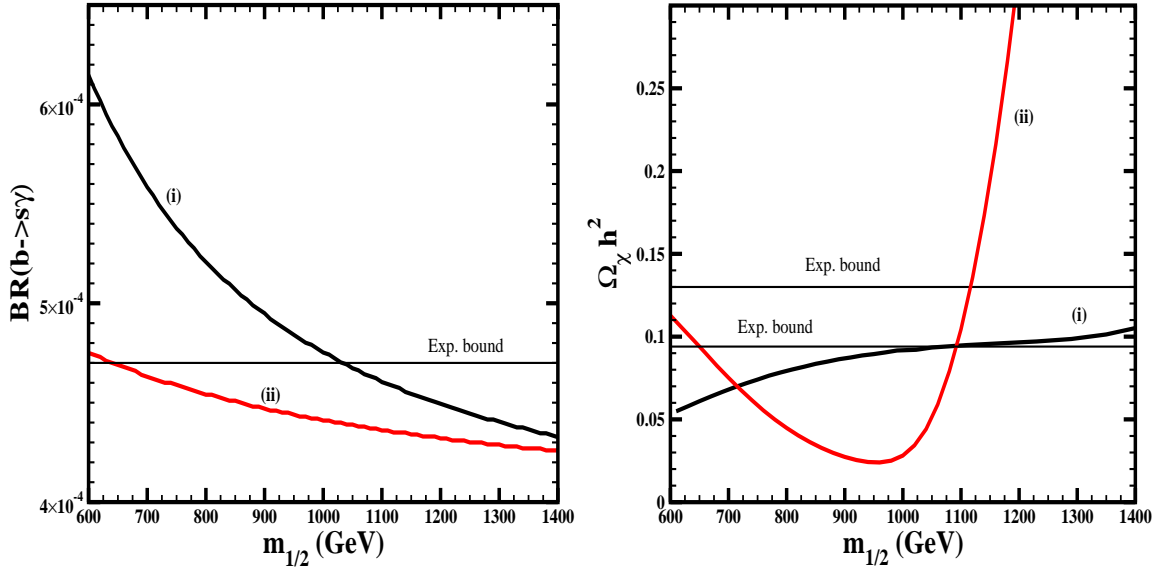


Figure 13: Analysis of the relic density and of $BR(b \rightarrow s\gamma)$ for the points in Table 1. For the case (i), m_0 is constrained to satisfy $m_0 = 0.832 \cdot m_{1/2}$ and in the case (ii), $m_0 = 1.8 \cdot m_{1/2}$.